[CANCER RESEARCH 59, 4770–4775, October 1, 1999]

Advances in Brief

Tumor Development under Angiogenic Signaling: A Dynamical Theory of Tumor Growth, Treatment Response, and Postvascular Dormancy[1]

Philip Hahnfeldt, Dipak Panigrahy, Judah Folkman, and Lynn Hlatky[2]

Department of Adult Oncology, Dana-Farber Cancer Institute and Joint Center for Radiation Therapy [P. H., L. H.], and Division of Pediatric Surgery, Children's Hospital [D. P., J. F.], Harvard Medical School, Boston, Massachusetts 02115

Abstract

The effects of the angiogenic inhibitors endostatin, angiostatin, and TNP-470 on tumor growth dynamics are experimentally and theoretically investigated. On the basis of the data, we pose a quantitative theory for tumor growth under angiogenic stimulator/inhibitor control that is both explanatory and clinically implementable. Our analysis offers a ranking of the relative effectiveness of these inhibitors. Additionally, it reveals the existence of an ultimate limitation to tumor size under angiogenic control, where opposing angiogenic stimuli come into dynamic balance, which can be modulated by antiangiogenic therapy. The competitive influences of angiogenically driven growth and inhibition underlying this framework may have ramifications for tissue size regulation in general.

Introduction

Conventional cancer treatment includes many modalities, all having the same basic intent: to directly kill tumor cells or prevent their proliferation. Accordingly, kinetic understanding of tumor control has focused on the elucidation of tumor cell proliferation and sensitivity characteristics. However, a tumor population is far from stable, manifesting with its genetic, epigenetic, and microenvironmental heterogeneity a constantly evolving spectrum of tumor cell expressions and behaviors. This raises the concern that current therapeutic attempts to target the expanding array of tumor expressions with customized molecular attacks may be overascribing durable and exploitable mechanistic bases to what are in fact largely temporal and hypervariable events. By contrast, therapy directed against tumor vasculature does not exploit tumor cell sensitivities, relying instead on tumor suppression consequent to inhibition of associated vasculature (1–5). By providing a means to control an exceptionally heterogeneous, unconstrained tumor population via a relatively homogeneous and constrained endothelial population, antiangiogenic therapy allows one to disregard a vast array of spatial and temporal details of tumor cell expression. Likewise, the power of a theoretical description of angiogenic control dynamics lies in its embrace of governing principles which provide insight into how such therapy may be implementable across tumor presentations, independent of tumor-specific details. Here we present experimental data from antiangiogenically treated and untreated Lewis lung tumors in mice and explain the data in terms of a customized quantitative model for tumor development under angiogenic stimulator and inhibitor control. Besides explaining tumor growth dynamics and quantifying the relative therapeutic effectiveness of the studied antiangiogenic agents, endostatin (6, 7) angiostatin (8, 9), and TNP-470 (10, 11), this analysis predicts that in principle there can exist a postvascular dormant state where stimulator and inhibitor come into balance and tumor growth is halted.

Materials and Methods

Tumor Cell Implant, Treatment, and Measurement. Male C57BL6/J mice (Jackson Labs, Bar Harbor, ME), 6–8 weeks of age, were used. For tumor implantation, mice were injected s.c. in the proximal dorsal midline with 1×10^6 Lewis lung carcinoma cells in 0.1 ml of saline. Tumor dimensions were measured with calipers. Volumes were calculated by taking width^2 $\times$ length $\times$ 0.52. After about 3–10 days, when tumor volumes were 100–300 mm^3, mice were randomized into four groups. Two groups received either recombinant mouse angiostatin (*Escherichia coli*; from Jie Lin) or mouse endostatin (*E. coli*; from Thomas Boehm) as a suspension in PBS. Mice in these groups were injected s.c. at a site distant from the tumor once daily. A third group received TNP-470 in saline injected s.c. every other day. The fourth group received injections of the vehicle alone.

Model Design. Our model departs from earlier theoretical constructs in that it considers an effective vascular support, or carrying capacity, for the tumor to be explicitly time dependent and under the control of distinct stimulatory and inhibitory angiogenic signals arising from the tumor. Others (12–14) have well-recognized the potential dynamic insights afforded by models that explicitly incorporate a vascular dependence to tumor growth. However, we sought to improve these characterizations in light of advances in the field by including a dynamic *versus* a static support, by freeing effective support levels from a strict dependence on tumor volume to render the theory more conducive to antiangiogenic therapy applications, and by limiting parameterization while still including explicit terms for the distinct actions of positive and negative angiogenic stimuli.

Model Curve Generation. Basic numerical integration with an interval resolution of 0.00001 day was used to plot the curve points. To solve for the model coefficients and fit the data, about 1,000,000 runs of a Monte-Carlo algorithm in each instance were used. Preliminary runs showed λ_2 to be negligible. On this basis, the algorithm was then used with progressively finer mesh resolution to solve for the values of λ_1, b, d, and k_0 (initial value of k) that minimized the squared error in the control fit (Fig. 1*A*). The treatment fits (Fig. 1, *B–D*) were likewise accomplished by similar minimizations over just the two agent parameters e (the vascular inactivation rate) and clr (the clearance rate; Table 1). Notably, the two predictive fits (Fig. 2) were accomplished with no free parameters.

Results and Discussion

Model of Stimulator/Inhibitor-dependent Tumor Growth. It is key that a contemporary theoretical depiction of tumor growth address the issues of: (*a*) providing a time-dependent carrying capacity under angiogenic control; (*b*) being minimally parameterized; and (*c*) recognizing the distinct kinetics for angiogenic stimulation and inhibition. Such an accounting of tumor/vascular interactions as modified by administered inhibitors thus forms a basis for both describing tumor development and for assessing antiangiogenic treatment alter-

Received 4/8/99; accepted 8/18/99.

The costs of publication of this article were defrayed in part by the payment of page charges. This article must therefore be hereby marked *advertisement* in accordance with 18 U.S.C. Section 1734 solely to indicate this fact.

[1] This work was supported by NIH Grant 1RO1-CA-78496 (to P. H.), a grant from the Gerry and Nancy Pencer Brain Trust (to L. H.), NCI Grant R01-CA-64481 (to J. F.), and a grant to Children's Hospital from Entremed, Inc.

[2] To whom requests for reprints should be addressed, at Department of Adult Oncology, JFB, Room 523, Dana-Farber Cancer Institute, Harvard Medical School, Boston, MA 02115. E-mail: Lynn_Hlatky@dfci.harvard.edu.

natives, alone or in combination with other conventional therapies (15, 16).

These notions were implemented beginning with the "generalized logistic" equation:

$$V' = PV \quad \text{where} \quad P = \lambda\left(1 - \left(\frac{V}{V_{\max}}\right)^{\alpha}\right) \tag{A}$$

This relationship equating the rate of change in tumor mass, V', to a decreasing factor P of tumor mass V captures the phenomenology of tumor growth slowdown to a hypothetical limiting size $V_{\max}$ as the tumor grows and ultimately taxes its available support. The finer details of the slowdown are incorporated into the exponent α and include for small α the familiar Gompertz form:

$$P = -\lambda\alpha\log\left(\frac{V}{V_{\max}}\right) \tag{B}$$

Gompertzian growth, as represented by Eqs. A and B, has come to be closely identified with the phenomenon of tumor growth slowdown with size widely observed both in the clinic and the laboratory for the past 100 years (17, 18).

We here propose that basic Gompertzian growth may be understood in terms of a bidirectional control process whereby a tumor regulates associated vascular growth or suppression, and the tumor vasculature in turn controls tumor growth through its usual nutritive function. We found that a derivative of Gompertz theory that formally includes these dynamic considerations presents a formalism that best explains the data and provides a template for quantitatively anticipating the effects of therapies seeking to use antiangiogenic agents. To arrive at this new theory, we reexamined the terms of the classic Gompertz model. Historically, the value $V_{\max}$ in Eq. B has been usefully thought of as a (fixed) sustenance level, or carrying capacity, for the tumor. But insofar as the tumor controls this level through factor secretions both stimulating and inhibiting vascular growth, we replaced this with a variable carrying capacity $K(t)$ and a dependence of the rate of change of K (K') on K, V, and t as follows:

$$V' = -\lambda_1 V\log\left(\frac{V}{K}\right), \quad K' = f(K, V, t) \tag{C1}$$

The carrying capacity K is defined as the effective vascular support provided to the tumor as reflected by the size of the tumor potentially sustainable by it. This definition is a measure of actual tumor sustenance and thus ignores that portion of the microcirculation that may be dysfunctional for a variety of reasons (19). It follows that $K = V$ at the point where it is just adequate to support the tumor, larger than V for growing tumors, and smaller than V for regressing tumors. Biological processes controlling the size of the effective vascular compartment include the intrinsic loss rate, stimulatory and inhibitory influences from the tumor cells, and inhibition due to administered inhibitors.

A form for $f(K, V, t)$, the terms of which are motivated by these four effects is:

$$f(K, V, t) = -\lambda_2 K + bS(V, K) - dI(V, K) - eKg(t) \tag{C2}$$

The first term represents the spontaneous loss of functional vasculature; the second term represents the stimulatory capacity of the tumor upon the inducible vasculature (through, *e.g.*, angiogenic factors like vascular endothelial growth factor; Ref. 20); the third term reflects endogenous inhibition of previously generated vasculature (through, *e.g.*, endothelial cell death or disaggregation); and the last term represents inhibition of tumor vasculature due to administered inhibitors, taken to be proportional to K and the concentration $g(t)$, as is typically done in chemotherapy models (21). The concentration of administered inhibitor $g(t)$ at a given time t generally includes partially cleared contributions from prior administrations across all earlier times $t' < t$. Under the usual pharmacokinetic assumptions, the expression for $g(t)$ is:

$$g(t) = \int_0^t c(t')\,\exp\,(-clr(t - t'))\,dt' \tag{C3}$$

where $c(t')$ is the rate of administration of inhibitor concentration at time t' and clr is the clearance rate.

The forms for $S(V, K)$ and $I(V, K)$ in Eq. C2 have yet to be established. Some insight into the forms of these terms comes, however, from arguments posed to explain the apparent inconsistency that a primary tumor can grow despite the production of inhibitory agents that are on occasion potent enough to render tumors at secondary sites dormant (22). It has been asserted that tumor-derived inhibitors from all sites act more systemically, whereas tumor-derived stimulators act more locally to the individual secreting tumor site (8), in turn suggesting that the persistences, or "half-lives," of endogenous inhibitors tend to greatly exceed those of endogenous stimulators. Where applicable, these arguments lead to certain restrictions on $S(V, K)$ and $I(V, K)$, as will next be demonstrated. One conclusion from the following is the assurance that, despite treating carrying capacity as variable, a classic Gompertz-like effect with regard to ultimate tumor growth can be expected.

To ascertain the natures of $S(V, K)$ and $I(V, K)$ and therefore of ultimate tumor growth, suppose we have a tumor of diameter $2r_0$ composed of cells secreting stimulator or inhibitor at a rate s_0, which is cleared at an exponential rate c. A diffusion-consumption equation for the concentration n of stimulator or inhibitor inside and outside the tumor may be written as follows:

$$D^2\nabla^2 n - cn + s = \frac{\partial n}{\partial t}$$

where D^2 is the diffusion coefficient, $s = s_0$ inside the tumor, and $s = 0$ outside.

Table 1 *Summary of kinetic model*

The kinetic model summarized by Eqs. C1, C2, C3, and C4, was applied first to the untreated control tumor data, and the growth parameters λ_1, λ_2, b, d, and k_0 (initial value of K) were solved for by performing about 1,000,000 runs of a Monte Carlo algorithm. Using the same growth parameters generated from the Gompertz fit, the data for TNP-470 (30 mg/kg/q.o.d.), endostatin (20 mg/kg/day) and angiostatin (20 mg/kg/day) were used to solve for the respective treatment parameters e and clr. (conc ≡ mg/kg; vol ≡ mm^3).

	e ($day^{-1}conc^{-1}$)	clr (day^{-1})	e/clr ($conc^{-1}$)	λ_1 (day^{-1})	λ_2 (day^{-1})	b (day^{-1})	d ($day^{-1}vol^{-2/3}$)	k_0 (initial K) (vol)
Control				0.192	0.0	5.85	0.00873	625
TNP-470	1.3	10.1	0.13	0.192[a]	0.0[a]	5.85[a]	0.00873[a]	625[a]
Endostatin	0.66	1.7	0.39	0.192[a]	0.0[a]	5.85[a]	0.00873[a]	625[a]
Angiostatin	0.15	0.38	0.39	0.192[a]	0.0[a]	5.85[a]	0.00873[a]	625[a]

[a] Growth parameters generated from the Gompertz fit.

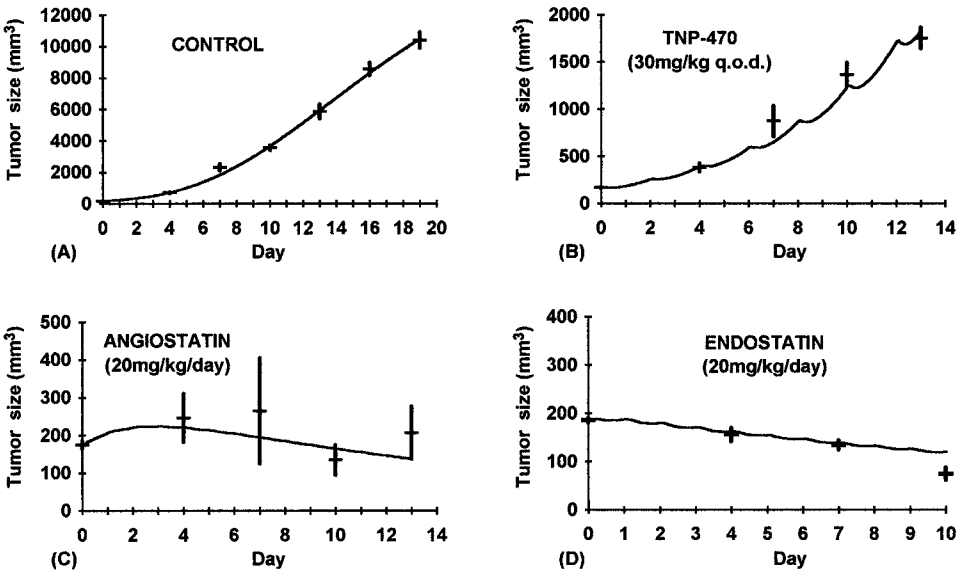

Fig. 1. Lewis lung carcinoma implanted in C57BL/6 mice. Treatment was initiated on day 0 (5 days after implantation) when tumors were ~200 mm^3 in size. Treatment regimens were 20 mg/kg/day. Tumors were measured on days 0, 4, and every third day thereafter. *A*, control data and the fitted model curve using Eqs. C1, C2, C3, and C4 with the parameters in Table 1. *B–D*, tumor response data and fitted curves to treatments with TNP-470 (*B*), angiostatin (*C*), and endostatin (*D*). The fits to the data were performed using the one-time fit of the model to the control and solving in each instance for the corresponding agent parameters, the vascular inhibition rate *e* and the clearance rate *clr*. *Data*, horizontal segment with *vertical error bars* (±1 SD); *curves*, model derived.

If we assume the tumor is in quasi-steady state, *i.e.*, that its growth rate is small relative to the rate of distribution of factor, then $\partial n \partial t = 0$. If we further assume radial symmetry, then $n = n(r)$, where r is the distance from the center of the tumor, the problem reduces to:

$$n'' + \frac{2n'}{r} - \frac{cn}{D^2} + \frac{s}{D^2} = 0$$

Making the substitutions (u, z) for (r, n), where $u = rc^{1/2}/D$ and $z = r^{1/2}(n - s/c)$, the result is a modified Bessel equation in $z(u)$ of order ½. The two fundamental solutions of this equation are:

$$z_1 = \frac{\sinh(u)}{\sqrt{u}} \quad \text{and} \quad z_2 = \frac{e^{-u}}{\sqrt{u}}$$

from which it can be shown, with the further definition $u_0 = r_0 c^{1/2}/D$, that the concentration n inside and outside the tumor is:

$$n_{\text{inside}}(r) = \frac{s_0}{c}\left(1 - (1 + u_0)e^{-u_0}\frac{\sinh(u)}{u}\right) \quad \text{and}$$

$$n_{\text{outside}}(r) = \frac{s_0}{c}\left(u_0\cosh(u_0) - \sinh(u_0)\right)\frac{e^{-u}}{u}$$

The two extremes of the clearance time c are now of interest. For small c (inhibitor case), *i.e.*, for $c \ll D^2/r_0^2$, we obtain:

$$n_{\text{inside}}(r, \text{ small } c) \approx \frac{s_0}{6D^2}(3r_0^2 - r^2) \quad \text{and}$$

$$n_{\text{outside}}(r, \text{ small } c) \approx \frac{s_0 r_0^3}{3D^2 r}$$

whereas for large c (stimulator case), we obtain:

$$n_{\text{inside}}(r, \text{ large } c) \approx \frac{s_0}{c} \text{ and } n_{\text{outside}}(r, \text{ large } c) \approx 0$$

It is clear, therefore, that inhibitor will impact on the target endothelial cells in the tumor in a way that grows ultimately as r_0^2 or $(Volume)^{2/3}$, whereas the impact of stimulator will be relatively independent of tumor/vascular size. It follows that, as r_0 increases, the effect of the inhibitor on tumor endothelial cells will overtake that of the stimulator, leading to a "plateau" in tumor size.

The model implication of this finding is that the inhibitor term of the expression for K' in Eqs. C1 and C2 will tend to grow at a rate $K^\alpha V^\beta$ faster than the stimulator term, where $\alpha+\beta \approx 2/3$, because both K and V have "volume" dimensions. If we now argue that the inhibitor term reflects tumor cells producing inhibitor that impacts on the vasculature K, then the final inhibitor term would become $dKV^{2/3}$, where, again, the $V^{2/3}$ factor reflects the r_0^2 dependence of the mean inhibitor source strength. A form for the stimulator, then, is immediately suggested to be $bKV^{2/3}/(K^\alpha V^\beta)$ or $bK^\gamma V^\delta$, where $\gamma + \delta \approx 1$. We chose bV to represent this term, although bK would be another arguable choice (the difference should not be dramatic because V and K tend to move together). The final form for the expression for K' in Eqs. C1 and C2) is:

$$K' = -\lambda_2 K + bV - dKV^{2/3} - eKg(t) \qquad \text{(C4)}$$

Eqs, C1, C2, C3, and C4 comprise the complete model formulation for tumor growth control under the actions of angiogenic stimulation and inhibition.

Antiangiogenic Treatment: Data and Analysis. The control and treatment data for three different inhibitors, demonstrating the effects of systemic administration of antiangiogenic agents on tumor growth through modulation of stimulator/inhibitor balance, are shown in Figs. 1 and 2. The accompanying curves show the corresponding tumor response as derived from the model. The inhibitors mouse endostatin (6, 7), mouse angiostatin (8, 9), and TNP-470 (10, 11) were tested against Lewis lung tumors grown in C57BL/6 mice. Treatment was initiated on day 0 (5 days after implantation) when tumors were ~200 mm^3 in size. Treatment regimens were 20 mg/kg/day and 4 mg/kg/day for endostatin, 20 mg/kg/day for angiostatin, and 30 mg/kg/q.o.d.[3] for TNP-470. Tumors were measured on day 0, day 4, and every third day thereafter. It is seen that treatment regimens of 20 mg/kg/day of either angiostatin or endostatin, or 20 mg/kg/day each of angiostatin and endostatin in combination, control Lewis lung tumor growth. The rate of regression for Lewis lung tumors treated with 20 mg/kg/day of endostatin is in agreement with the published results of Boehm *et al.* (6), where full regressions were observed after this treatment. By

[3] The abbreviation used is: q.o.d., every second day.

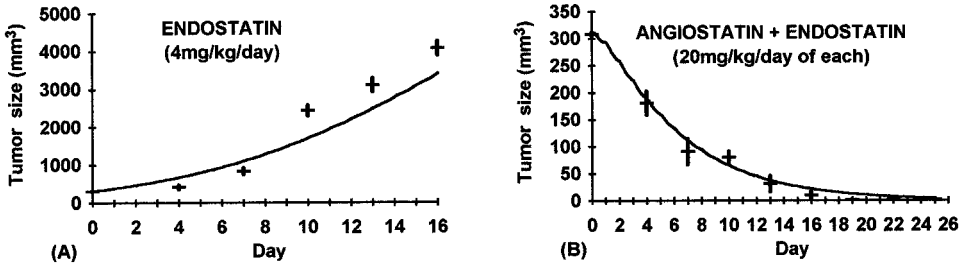

Fig. 2. The curves overlying the endostatin (4 mg/kg/day) data (*A*) and the combined angiostatin and endostatin data (20 mg/kg/day of each; *B*) are parameter-free theoretical predictions of tumor response based on the inhibition and clearance rates derived previously for the endostatin (20 mg/kg/day) and angiostatin (20 mg/kg/day) data separately. Excellent agreement of predictions to data is observed.

contrast, 30 mg/kg/q.o.d. of TNP-470 or 4 mg/kg/day of endostatin does not control the growth of these tumors.

The model given by Eqs. C1, C2, C3, and C4 was used to analyze this data. Inhibitors were administered as boli, meaning that $c(t')$ in the model Eq. C3 was taken to be $D(\delta(t' - t_1) + \delta(t' - t_2) + \delta(t' - t_3) + \dots)$, where D is the dose concentration administered and the t_i are the injection days. An excellent control fit was obtained (Fig. 1*A*), solving for the parameters λ_1, λ_2, b, and d. The parameter λ_2 was found to be negligible, *i.e.*, constitutive endothelial cell loss does not play a major role in this system. The good fits to treatment data (Fig. 1, *B–D*) with the two available treatment parameters e and clr support the underlying model of tumor/endothelial interaction and growth dynamics. The values e, the vascular inactivation rate, and clr, the agent clearance or inactivation rate, together offer a measure of the antiangiogenic effectiveness per unit concentration, one estimate being e/clr (see Table 1) because by Eq. C4, we expect that a bolus dose of an antiangiogenic agent will cause a factor reduction in K by $\exp(-e/clr)$. Under this scheme, the inhibitors TNP-470, endostatin, and angiostatin have relative effectiveness of 0.13, 0.39, and 0.39, respectively.

Importantly, the parameters inferred from the data (Table 1) had predictive power for two additional experiments (Fig. 2). The close agreement of the parameter-free theoretical projections with data for endostatin (4 mg/kg/day; Fig. 2*A*) and for angiostatin/endostatin in combination (20 mg/kg/day of each; Fig. 2*B*) support model assumptions that these agents act linearly (*i.e.*, exponentially with instantaneous concentration) and together act additively upon the vasculature. An additive vascular response for endostatin and angiostatin in combination would suggest that either the combined 40 mg/kg dose size is still below threshold for target saturation or the modes of action of angiostatin and endostatin are different.

The effective tumor-associated vasculature is represented by the carrying capacity in the kinetic formulation (*red curves* in Figs. 3 and 4*A*). For the untreated tumor, this vascular component is predicted to first increase more rapidly than the tumor cell population, reaching a point where V/K is at a minimum and tumor growth is most rapid (Fig. 4*A*). As the tumor continues to grow, however, V/K increases asymptotically to one, and tumor growth slows to zero. For treated tumors, it is apparent that the endothelial compartment is highly responsive to the administered inhibitors, with subsequent tumor response being comparatively slower. Fluctuations in effective vasculature occur because of the saltatory nature of the administration of inhibitor. The fluctuations in effective vascularity are most dramatic with TNP-470 (Fig. 3*B*), because of a high potency combined with an exceptionally fast clearance rate. Although this model-derived clearance rate is very rapid at 10.1 day^{-1}, it is still less than the 18.9 day^{-1} rate (equivalent to a terminal half-life of 0.88 h) determined for TNP-470 by pharmacokinetic methods in patients being treated for HIV-associated Kaposi's sarcoma (11). Aside from the obvious host differences, the discrepancy may in large part be due to the fact that TNP-470 has active metabolites, including AGM-1883, that escape strict pharmacokinetic assay for TNP-470 but nonetheless take part here in suppressing vasculature.

The comparative speed of vascular response *versus* tumor response to these inhibitors raises the concern that some of the potency of dosing is "wasted" through unproductively oscillating the vasculature over the course of treatment (*e.g.*, Fig. 3, *B* and *C*). Arguably, delivering the same integrated dose more continuously over the treatment period would maintain a steadier vascular response and give better results. Our model reveals this effect. For example, with TNP-470 delivered at 30 mg/kg/q.o.d. *versus* continuously at the same integrated dose, the tumor size at day 13 is predicted to be 1840 mm^3 *versus* 1300 mm^3, respectively (data not shown).

Stimulator/Inhibitor Balance under Antiangiogenic Treatment Determines Tumor "Set Point." Apart from enabling quantifications and comparisons of inhibitor effectiveness, this analysis demonstrates a principle of tumor growth control the qualitative features of which transcend treatment details. Predicted in general is the tendency for tumors to show growth deceleration with size. Under sufficient treatment, and in some cases naturally, tumor size is projected to plateau as a result of a parallel plateauing of available vascular support. The latter happens as a result of the eventual offsetting of vascular stimulation by a more rapidly rising level of

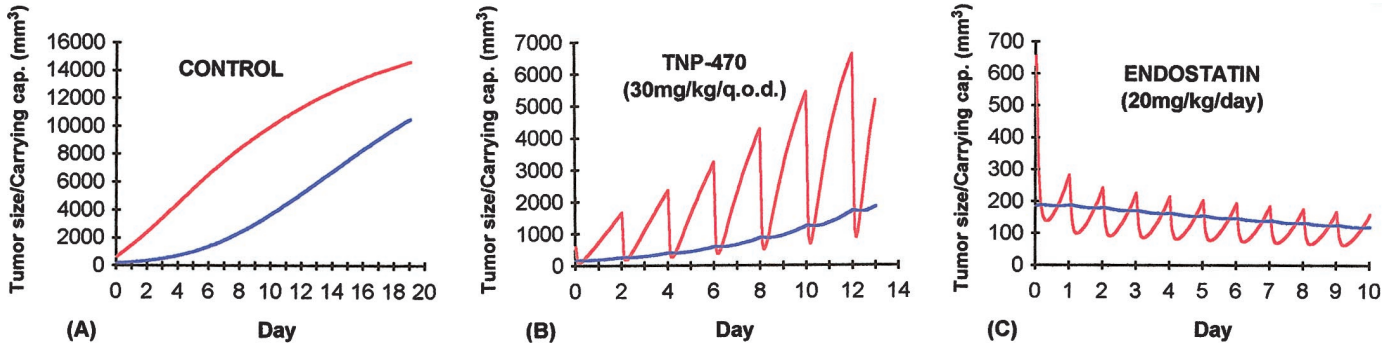

Fig. 3. Tumor growth (*blue*) with model predictions of the accompanying net vascular support size (*red*) for the untreated control tumor population (*A*) and for tumors treated with TNP-470 (30 mg/kg/q.o.d.; *B*) and endostatin (20 mg/kg/day; *C*). Following administration of inhibitor, the vasculature regressed. Between injections, net vascular recovery is predicted to be comparatively rapid, particularly for TNP-470 because of its exceptionally fast clearance rate.

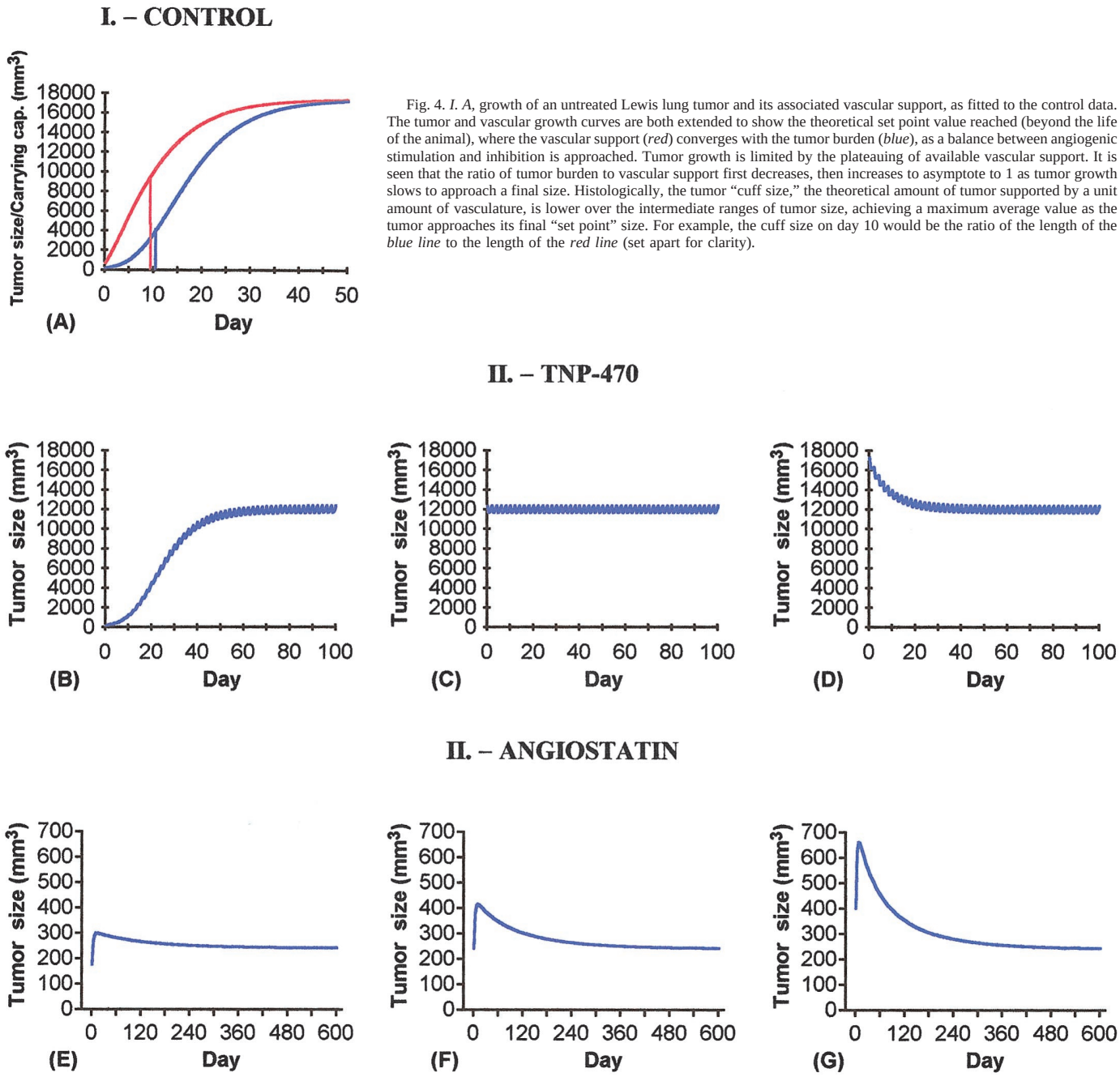

Fig. 4. *I. A*, growth of an untreated Lewis lung tumor and its associated vascular support, as fitted to the control data. The tumor and vascular growth curves are both extended to show the theoretical set point value reached (beyond the life of the animal), where the vascular support (*red*) converges with the tumor burden (*blue*), as a balance between angiogenic stimulation and inhibition is approached. Tumor growth is limited by the plateauing of available vascular support. It is seen that the ratio of tumor burden to vascular support first decreases, then increases to asymptote to 1 as tumor growth slows to approach a final size. Histologically, the tumor "cuff size," the theoretical amount of tumor supported by a unit amount of vasculature, is lower over the intermediate ranges of tumor size, achieving a maximum average value as the tumor approaches its final "set point" size. For example, the cuff size on day 10 would be the ratio of the length of the *blue line* to the length of the *red line* (set apart for clarity).

Fig 4. II. The set point attained by ongoing treatment is independent of the tumor volume at which treatment is initiated, depending only on how the ongoing treatment modulates the balance between angiogenic stimulators and inhibitors. The set point is determined by the point in tumor growth where stimulation and inhibition (from both endogenous and therapeutic sources) come into balance. *TNP-470*, the effect of beginning a TNP-470 regimen (30 mg/kg/q.o.d.) at day 0 (tumor size ~170 mm^3) on the control tumor modifies the course of growth, limiting the final size to 12,300 mm^3 (*B*). This final value is not sensitive to treatment start time but, rather, is determined by the average extent to which the administered inhibitor supplements endogenous inhibition. If treatment commences instead when the tumor size is already 12,300 mm^3, the tumor will remain at that size (*C*). Likewise, if treatment commences at a time when the tumor size is larger than this asymptotic value (example shown: $V = 17{,}300$ mm^3), treatment brings the tumor down to, but not beyond, the asymptotic set point size $V = 12{,}300$ mm^3 (*D*). *ANGIOSTATIN*, on the basis of the angiostatin response with 20 mg/kg/day, a calculated response to 14 mg/kg/day is shown. This dose level is insufficient to accomplish a complete regression. Instead, tumor size is driven toward a finite set point value. By starting treatment at the same 177 mm^3 tumor size as for the 20 mg/kg/day experiment, tumor size is seen to first rise, then settle back to a set point value of ~240 mm^3 (*E*). The consequence of initiating treatment at a later time when tumor size has reached 240 mm^3 is shown (*F*). Although the tumor continues to grow for a time under treatment (~10 days), it then regresses back to the 240-mm^3 set point size as before. *G*, consequence of starting treatment at a still larger tumor size, in this case, 400 mm^3. An initial overshoot is once again observed before final asymptotic descent to the 240-mm^3 set point. The rise and subsequent downturn in each instance is attributable to the accumulation of dose concentration as the regimen proceeds, an effect arising from the relatively slow clearance of this agent.

vascular inhibition arising from the tumor. Administered antiangiogenic agents act to generate lower plateau points. Although the predicted plateau size for a naturally plateauing tumor may be too large to be compatible with the viability of the host, antiangiogenic treatments offer the prospect of reducing the asymptotic "set point" to a clinically tolerable level (Fig. 4). Such a tumor, held in check due to its stimulator/inhibitor balance, would be dormant yet vascularized. This is distinct from the prevascular dormant state (9) tumors advance through in the process of becoming full-fledged cancers.

As examples of the tumor set point and its modulation by therapy, Fig. 4*A* shows the growth slowdown and asymptotic limit (~17400 mm^3) of Lewis lung tumor size that would hypothetically be reached

if this size of tumor were compatible with the life of the animal. As this set point size is approached, the effective vasculature shows less potential to support further tumor growth, as indicated by the gradual merging of the tumor size (*blue*) and carrying capacity (*red*) curves. It is seen that the ratio of tumor burden to vascular support first decreases, then increases to asymptote to unity as tumor growth slows to approach a final size. Extrapolating both the TNP-470 (30 mg/kg/q.o.d.) treatment regimen and a theoretical angiostatin regimen (14 mg/kg/day) predicted by the model based on the angiostatin (20 mg/kg/day) data, it is seen that the expected result of continued treatment in each instance is a fixed final tumor size where stimulatory and inhibitory influences on the associated vasculature come into balance. Importantly, these final tumor sizes are independent of the size of the tumor at the time treatment is initiated. Specifically, for treatment with TNP-470, there is a monotonic ascent or descent to the same final tumor volume, or set point, of $\sim$12300 mm^3, whether treatment is started at a volume smaller than 12,300 mm^3 (Fig. 4*B*), at the same volume (Fig. 4*C*), or at a larger volume (Fig. 4*D*). The calculated angiostatin protocol (14 mg/kg/day) shows the same tendency to approach a fixed final size (240 mm^3) irrespective of initial size, but in this case it shows first a brief period of overshoot growth (Fig. 4, *E–G*). Notably, in the clinic, such a growth overshoot could be prematurely interpreted as nonresponsiveness to treatment. It may thus be important to establish tailored treatment progress criteria for agents that suppress tumor growth indirectly by way of inhibiting the associated neovascularization.

The results here indicate the ubiquitous tendency of tumors to exhibit a growth slowdown with a possible asymptotic approach to a final tumor size, or "set point." We show this may be understood in terms of the net angiogenic influence upon the tumor becoming more inhibitory over time, independent of any tumor cell-specific details. This growth limitation may well be a distorted recapitulation of the rules governing ultimate organ size in organogenesis. Developing tumors and organs may share an awareness of total mass through the exertion of an increasingly inhibitory influence on their own growths by way of increased natural angiogenic suppression, even to the point of reaching a critical size where further growth is actively self-inhibited. As a rule, naturally occurring tumor set points likely occur too late in patients to prevent morbidity and mortality. The advantage of antiangiogenic therapy may lie in its ability to alter this course by creating set points at small or even vanishing tumor sizes.

Summary. We have developed a quantitative theory of tumor growth and treatment response under angiogenic stimulator and inhibitor control. This theory is clinically implementable, offering a means of ranking of angiogenic inhibitors and suggesting a trend to better dose response with more continuous dosing. Predicted is the potential attainment of a growth plateau (set point) resulting from a dynamic balance between angiogenic stimulation and inhibition that can be modulated by antiangiogenic therapy.

Acknowledgments

We thank Ray Sachs and Michael O'Reilly for valuable discussions, Thomas Boehm for murine endostatin, and Jie Lin for murine angiostatin.

References

1. Folkman, J. Clinical applications of research on angiogenesis. N. Engl. J. Med., *333:* 1757–1763, 1995.
2. Folkman, J., Hahnfeldt, P., and Hlatky, L. The logic of anti-angiogenic gene therapy. *In:* T. Friedmann (ed.), The Development of Gene Therapy, pp. 1–17. Cold Spring Harbor, NY: Cold Spring Harbor Laboratory, 1998.
3. Denekamp, J. Vascular attack as a therapeutic strategy for cancer. Cancer Metastasis Rev., *9:* 267–282, 1990.
4. Kerbel, R. S. Inhibition of tumor angiogenesis as a strategy to circumvent acquired resistance to anti-cancer therapeutic agents. BioEssays, *13:* 31–36, 1991.
5. Arap, W., Pasqualini, R., and Ruoslahti, E. Chemotherapy targeted to tumor vasculature. Curr. Opin. Oncol., *10:* 560–565, 1998.
6. Boehm, T., Folkman, J., Browder, T., and O'Reilly, M. S. Antiangiogenic therapy of experimental cancer does not induce acquired drug resistance. Nature (Lond.), *390:* 404–407, 1997.
7. O'Reilly, M. S., Boehm, T., Shing, Y., Fukai, N., Vasios, G., Lane, W. S., Flynn, E., Birkhead, J. R., Olsen, B. R., and Folkman, J. Endostatin: an endogenous inhibitor of angiogenesis and tumor growth. Cell, *88:* 277–285, 1997.
8. O'Reilly, M. S., Holmgren, L., Shing, Y., Chen, C., Rosenthal, R. A., Moses, M., Lane, W. S., Cao, Y., Sage, E. H., and Folkman, J. Angiostatin. A novel angiogenesis inhibitor that mediates the suppression of metastases by a Lewis lung carcinoma. Cell, *79:* 315–328, 1994.
9. O'Reilly, M. S., Holmgren, L., Chen, C., and Folkman, J. Angiostatin induces and sustains dormancy of human primary tumors in mice. Nat. Med., *2:* 689–692, 1996.
10. Ingber, D., Fujita, T., Kishimoto, S., Sudo, K., Kanamaru, T., Brem, H., and Folkman J. Synthetic analogues of fumagillin that inhibit angiogenesis and suppress tumour growth. Nature (Lond.), *348:* 555–557, 1990.
11. Figg, W. D., Pluda, J. M., Lush, R. M., Saville, M. W., Wyvill, K., Reed, E., and Yarchoan, R. The pharmacokinetics of TNP-470, a new angiogenesis inhibitor. Pharmacotherapy, *17:* 91–97, 1997.
12. Liotta, L. A., Saidel, G. M., and Kleinerman, J. Diffusion model of tumor vascularization and growth. Bull. Math. Biol., *39:* 117–128, 1977.
13. Michelson, S., and Leith, J. T. Positive feedback and angiogenesis in tumor growth control. Bull. Math. Biol., *59:* 233–254, 1997.
14. Balding, D., and McElwain, D. L. A mathematical model of tumour-induced capillary growth. J. Theor. Biol., *114:* 53–73, 1985.
15. Mauceri, H. J., Hanna, N. N., Beckett, M. A., Gorski, D. H., Stellato, N., Bigelow, K., Heimann, R., Gately, S., Dhanabell, M., Soff, G. A., Sukhatmell, V. P., Kufe, D. W., and Weichselbaum, R. R. Combined effects of angiostatin and ionizing radiation in anti-tumour therapy. Nature (Lond.), *394:* 287–291, 1998.
16. Teicher, B. A., Holden, S. A., Ara, G., Korbut, T., and Menon, K. Comparison of several antiangiogenic regimens alone and with cytotoxic therapies in the Lewis lung carcinoma. Cancer Chemother. Pharmacol., *38:* 169–177, 1996.
17. Skehan, P. On the normality of growth dynamics of neoplasms *in vivo*: a data base analysis. Growth, *50:* 496–515, 1986.
18. Spratt, J. S., Meyer, J. S., and Spratt, J. A. Rates of growth of human neoplasms: part II. J. Surg. Oncol., *61:* 68–83, 1996.
19. Dewhirst, M. W. Concepts of oxygen transport at the microcirculatory level. Semin. Radiat. Oncol., *8:* 143–150, 1998.
20. Hlatky, L., Hahnfeldt, P., Tsionou, C., and Coleman, C. N. VEGF. Environmental controls and effects in angiogenesis. A review. Br. J. Cancer, *74* (Suppl. XXVII)*:* S151–S156, 1996.
21. Skipper, H. E. On mathematical modeling of critical variables in cancer treatment (goals: better understanding of the past and better planning in the future). Bull. Math. Biol., *48:* 253–278, 1986.
22. Prehn, R. T. Two competing influences that may explain concomitant tumor resistance. Cancer Res., *53:* 3266–3269, 1993.